THE JOURNAL OF PHYSICAL CHEMISTRY A

Article

pubs.acs.org/JPCA

Theoretical Investigation of Interaction of Dicarboxylic Acids with Common Aerosol Nucleation Precursors

Wen Xu[†] and Renyi Zhang*[,†,‡]

[†]Department of Chemistry and [‡]Department of Atmospheric Sciences, Texas A&M University, College Station, Texas 77840, United States

Supporting Information

ABSTRACT: Dicarboxylic acids are important products from photooxidation of volatile organic compounds and are believed to play an important role in the formation and growth of atmospheric secondary organic aerosols. In this paper, the interaction of five dicarboxylic acids, i.e., oxalic acid ($C_2H_2O_4$), malonic acid ($C_3H_4O_4$), maleic acid ($C_4H_4O_4$), phthalic acid ($C_8H_6O_4$), and succinic acid ($C_4H_6O_4$), with sulfuric acid and ammonia has been studied, employing quantum chemical calculations, quantum theory of atoms in molecules (QTAIM), and the natural bond orbital (NBO) analysis methods. Several levels of quantum chemical calculations are considered, including coupled-cluster theory with single and double excitations with perturbative corrections for the triple excitations (CCSD(T)) and two density functionals, B3LYP and PW91PW91. The free energies of formation of the heterodimer and heterotrimer clusters suggest that dicarboxylic acids can contribute to the aerosol nucleation process by binding to sulfuric acid and ammonia. In particular, the formation energies and structures of the heterotrimer clusters show that dicarboxylic acids enhance nucleation in two directions, in contrast to monocarboxylic acids.

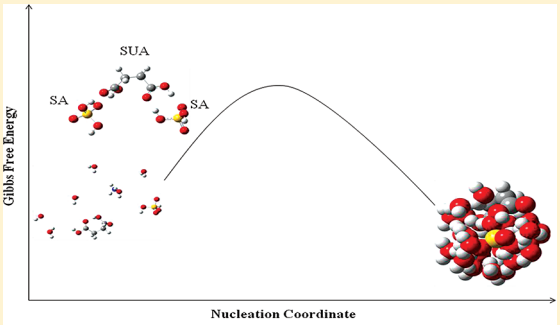

Atmospheric Aerosol Nucleation

1. INTRODUCTION

Atmospheric aerosols impact the Earth−atmosphere system in several aspects, i.e., influencing the Earth radiation budget, cloud formation, human health, photochemical chemistry, and partitioning of trace species by providing surfaces for heterogeneous chemical reactions.[1−6] The effects of aerosols are recognized as one of the key issues in the climate system and the hydrological cycle. Atmospheric aerosols cool the atmosphere by directly scattering a fraction of the incoming solar radiation back to space, which is often referred to as the aerosol direct effect. While acting as cloud condensation nuclei (CCN) and ice nuclei (IN), aerosols play an important role in controlling cloud formation, development and precipitation on local, regional and global scales,[1,3] which is often referred to as the aerosol indirect effect. Presently, the aerosol direct and indirect effects represent the largest uncertainty in climate predictions.[1]

Aerosols can be directly emitted into the atmosphere from natural and anthropogenic sources or formed in the atmosphere through nucleation from gas-phase species. New particle formation produces a large fraction of atmospheric aerosols and has been frequently observed in various environments, including urban, forested, and remote continental areas. New particle formation occurs in two distinct stages,[7−10] i.e., nucleation to form the critical nucleus (with the maximum free energy) and subsequent growth of the critical nucleus to a detectable size (2−3 nm) that competes with capture and removal of the critical cluster by coagulation with pre-existing aerosols. New particle formation is kinetically limited by the population of critical nucleuses; the rate at which nucleation occurs is related to the chemical makeup of the critical nucleus and the gaseous concentrations of the nucleating species and represents an important variable in simulations of aerosol formation in atmospheric models.[7] Currently, a large uncertainty exists in the chemical compositions of the critical nucleus and the identity of chemical species that participate in the nucleation and growth of nanoparticles in the atmosphere.

Several mechanisms have been proposed to explain nucleation events in the continental troposphere, including binary H_2SO_4/H_2O and ternary $H_2SO_4/H_2O/NH_3$ nucleation,[11,12] ion-mediated nucleation,[13,14] and nucleation enhanced by organic compounds.[15−17] Sulfuric acid has been widely identified as one of the major atmospheric nucleating species.[7,18] The importance of organic species in aerosol nucleation has been recently realized.[15−17,19,20] Organic compounds from anthropogenic and biogenic emissions react with atmospheric oxidants to form a number of products,[21−23] including organic carbonyls and acids, some of which may participate in nucleation and growth to form nanoparticles under various environments.[8,24,25] Organic aerosol nucleation

Received: February 28, 2012
Revised: April 3, 2012
Published: April 3, 2012

   dx.doi.org/10.1021/jp301964u | J. Phys. Chem. A 2012, 116, 4539−4550

was first suggested to occur through the formation of stable heterodimers of monocarboxylic acids.[26] However, theoretical calculations have indicated that those dimers have no vacant hydrogen acceptor/donor groups to promote subsequent cluster growth and are unlikely to contribute to new particle formation by themselves only.[7,17,20] On the other hand, the presence of organic acids considerably enhances new particle formation of the water-sulfuric acid system via formation of strongly hydrogen-bonded clusters containing one molecule of an organic acid and several molecules of sulfuric acid and water,[7,17,20,27] likely explaining field measurements of high aerosol concentrations observed in polluted and forested environments.

Numerous experimental and theoretical studies have been conducted to investigate the mechanisms of atmospheric aerosol nucleation. For example, previous theoretical studies using quantum chemical calculations have explored the interaction of sulfuric acid with ammonia,[28,29] amines,[30−32] and organic acids.[15,17,19,20,33−36] Strong hydrogen bonding between organic acids and atmospheric nucleation precursors has been demonstrated in the previous studies.[15,19,20] For example, Zhao et al. employed the quantum theory of atoms in molecules to elucidate the nature of hydrogen bonds formed in the organic acid clusters,[20] and the results indicated that the organic acids-sulfuric acid/ammonia clusters possess one strong-strength hydrogen bond and one medium-strength hydrogen bond, stabilizing the critical nucleus by lowering the free energy. In addition to monocarboxylic acids, theoretical studies on the interaction between dicarboxylic acids and common aerosol nucleation precursors have also been carried out for both neutral[33−35] and charged[34−36] clusters. Xu et al. showed that maleic acid stabilizes both neutral and ionic sulfuric acid/ammonia clusters,[34] whereas oxalic acid stabilizes only ionic clusters.[35] Ehn et al. showed that oxalic, malonic, and succinic acids stabilize anionic clusters of bisulfate.[36] Another previous study revealed that dicarboxylic acids have lower saturation vapor pressures than those of monocarboxylic acids,[37] suggesting that dicarboxylic acids may play a more important role in partitioning into the particle phase.

In the present study, the interaction of five dicarboxylic acids, including oxalic acid (OA, $C_2H_2O_4$), malonic acid (MOA, $C_3H_4O_4$), maleic acid (MEA, $C_4H_4O_4$), phthalic acid (PA, $C_8H_6O_4$), and succinic acid (SUA, $C_4H_6O_4$), with common atmospheric aerosol nucleation precursors (i.e., sulfuric acid and ammonia) is studied using the density functional theory (DFT), quantum theory of atoms in molecules (QTAIM), and natural bond orbital (NBO) analysis methods. The five dicarboxylic acids are chosen because they correspond to the most abundant dicarboxylic acids in the atmosphere.[38] The results of quantum chemical calculations using several different levels of theory, including coupled-cluster theory with single and double excitations with perturbative corrections for the triple excitations (CCSD(T)) and two density functionals, B3LYP and PW91PW91, are compared and discussed. The implications of the present results for atmospheric aerosol nucleation are discussed.

2. THEORETICAL METHODS

All the calculations were performed on a 3 64-core Altix 450 machines with 128GB memory each using Gaussian 03 software package.[39] B3LYP functional with Pople's basis set 6-311++G (2d, 2p) was employed for geometry optimization. For each stationary point, frequency calculations were performed to ensure there were no imaginary frequencies. The optimized geometry was taken in single point energy calculations using CCSD(T)) and PW91PW91 with the 6-311++G(2d,2p) and 6-311++G(3df,3pd) basis sets, respectively. Basis set superposition errors (BSSEs) at the B3LYP level of theory for each stationary point, and at PW91PW91 and CCSD(T) for some of the stationary points, were obtained using the counterpoise method implemented in Gaussian 03 package. The free energy of the cluster formation was calculated using the single point electronic energies from B3LYP, CCSD(T), and PW91PW91 and the thermal correction from B3LYP and BSSE corrections. The energetics of the sulfuric acid−water and oxalic acid−water clusters obtained at the B3LYP/6-311++G(2d,2p)) level was compared with the results from CCSD(T) and PW91PW91/6-311++G(3df,3pd). Subsequently, the geometry and energetics at the B3LYP/6-311++G(2d,2p) level was used to investigate the heterodimer and heterotrimer clusters of all dicarboxylic acids with sulfuric acid, ammonia, and water. In addition, single point calculations using PW91PW91/6-311++G(3df,3pd) were also made for comparison. To further evaluate the theoretical method, the results from B3LYP were compared with those reported previously using PW91PW91 for SA, OA, and MEA.[31,32]

The topological analysis of OA, MOA, MEA, PA, SUA, and clusters of PA with sulfuric acid, ammonia, and water was carried out using QTAIM[40] with AIM2000 software[41−43] at the B3LYP/6-311++G(2d,2p) level. The topological properties (e.g., charge density and its Laplacian, energy densities) at the hydrogen bond critical points were used to evaluate the individual hydrogen bond strength in those molecules and molecular clusters. NBO analysis[44] calculations were also carried out using Gaussian 03 to investigate the individual hydrogen bond strength.

3. RESULTS AND DISCUSSION

3.1. Geometrical Analysis. The geometries of H_2SO_4, H_2O, NH_3, and the five dicarboxylic acids are optimized at the B3LYP level with the 6-311++G(2d,2p) basis set using the Gaussian 03 package. The calculated geometries of H_2SO_4, H_2O, and NH_3 are consistent with the available experimental values (Supporting Information, Tables S1 and S2). Sulfuric acid possesses a C_2 symmetry, consistent with that described by Zhao et al.[20] There are several possible conformations of dicarboxylic acids and their molecular complexes, but only the conformations with the intramolecular O—H···O hydrogen bonds are presented. Figure 1 shows that, except for oxalic acid, the stable conformations of dicarboxylic acids have an intramolecular hydrogen bond and a free carboxylic group. An additional hydrogen bond is formed between the two adjacent carboxylic groups in oxalic acid. The strength of the intramolecular hydrogen bond is restrained by the molecular structure of the dicarboxylic acids. With a stronger hydrogen bond (i.e., a shorter O—H···O distance), lengthening of the O—H bond in the carboxylic group is larger. For example, the sequence of the intramolecular hydrogen bond distances of the five dicarboxylic acids in a decreasing order is OA (2.128 Å) > SUA (1.835 Å) > MOA (1.778 Å) > MEA (1.651 Å) > PA (1.598 Å), and the hydrogen bond strength increases correspondingly from OA to PA. In contrast, the sequence of the O—H bond lengths in the carboxylic group in an increasing order is OA (0.974 Å) < SUA (0.976 Å) < MOA (0.980 Å) < MEA (0.986 Å) and PA (0.986 Å). The O—H bond length in

dx.doi.org/10.1021/jp301964u | J. Phys. Chem. A 2012, 116, 4539−4550

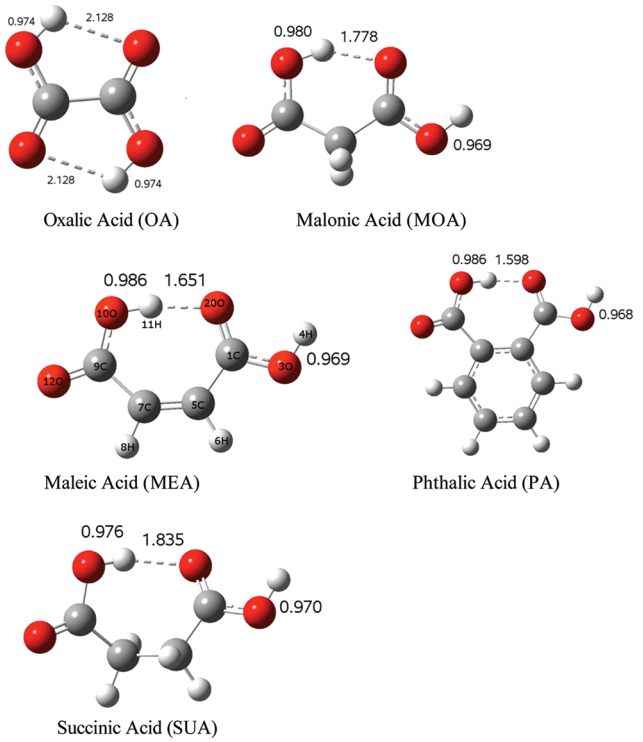

Figure 1. Optimized geometries of the five dicarboxylic acids at B3LYP/6-311++G(2d,2p) (red for oxygen, white for hydrogen, gray for carbon, yellow for sulfur, and blue for nitrogen).

the free carboxylic acid group ranges from 0.968 to 0.970 Å, which is shorter than the corresponding O—H bond length in the hydrogen bonded ones (0.974−0.986 Å).

The geometries obtained using B3LYP/6-311++G(2d,2p) for OA and MEA is summarized in Table 1, along with those previously reported using PW91PW91/6-311++G(3df,3pd) and the experimental values. Table 1 shows that both B3LYP and PW91PW91 geometries agree well with the experimental values. Table 2 compares the B3LYP and PW91PW91 vibrational frequencies of MEA with the experimental values. Similarly, both B3LYP and PW91PW91 yield the vibrational frequencies in agreement with the experimental values.

A previous study showed that succinic acid has two stable conformations, with and without intramolecular hydrogen bond.[45] The two conformations have a small energy difference of about 2.5 kcal mol^{-1} and convert readily to each other if the thermal kinetic energy is sufficient to facilitate crossing of this isomerization barrier. To obtain the potential energy surface (PES) along the reaction coordinate corresponding to breaking of the intramolecular hydrogen bond, a relaxed PES profile is obtained. The relative energies of the two conformations are plotted as a function of the intramolecular hydrogen bond length in Figure 2. The barrier height for isomerization between the two conformations is about 3 kcal mol^{-1} from configuration I to II. At room temperature (298.15 K), the translational energy is 1.5 kT, which equals 3.7 kcal mol^{-1}. As a result, thermal collision with buffer gas molecules at room temperature is sufficient to break the intramolecular hydrogen bond in succinic acid and conversion between the conformations occurs readily in the atmosphere.

On the basis of the monomers with one intramolecular hydrogen bond, the heterodimer molecular complexes of the dicarboxylic acids are constructed and optimized. Figure 3 illustrates the structures of the heterodimer complexes of PA with sulfuric acid/ammonia/water. There exists a pair of intermolecular hydrogen bonds between one of the carboxylic groups and sulfuric acid/ammonia/water and an intramolecular hydrogen bond for the additional carboxylic group. The PA molecule acts as both a hydrogen bond donor and acceptor in the intermolecular pair, with a stronger and a weaker hydrogen bond. Because the stronger hydrogen bond for the PA−ammonia (AM) complex involves the interaction of an nitrogen and hydrogen atom, the strength of this hydrogen bond cannot be directly compared to that of the PA−sulfuric acid (SA) complex using the bond lengths (i.e., 1.687 and 1.656 Å, respectively). Instead, the strength of the intermolecular hydrogen bond can be inferred from the lengthening of the adjacent O—H bond. The strength of the stronger intermolecular hydrogen bond decreases in the order from PA-AM (1.016 Å) to PA-SA (1.000 Å) to PA−water (W) (0.991 Å). Therefore, without considering the contribution from the weak hydrogen bond, the interaction between dicarboxylic acids and sulfuric acid/ammonia/water decreases from PA-AM to PA-SA to PA-W. However, for the weaker hydrogen bond, the strength of the PA-SA complex is the strongest (1.715 Å), and the strength of the PA-AM complex is the weakest (2.688 Å). The strength of the weaker hydrogen bond decreases from 1.715 Å for PA-SA to 2.169 Å for PW-W, consistent with lengthening of the adjacent O—H bond (i.e., from 0.989 to 0.968 Å, respectively). As discussed in the Topological and NBO Analysis and Thermochemical Analysis sections, the overall interaction energy can be computed from the combined strengths of the intermolecular hydrogen bond pair.

It is also interesting to compare the changes in the intramolecular hydrogen H···O bond, when a molecule of sulfuric acid/ammonia/water is added to the dicarboxylic acids. The strength of intramolecular hydrogen bond in PA-SA is weaker than that in PA. The adjacent O—H distance in PA-SA (0.980 Å) is shorter than that in PA (0.986 Å), whereas the intramolecular hydrogen bond distance in PA-SA (1.644 Å) is larger than that in PA (1.598 Å), both indicating a stronger bond for PA. This behavior is explained by the strong hydrogen donor characteristic of sulfuric acid. Because the oxygen atom (O═C in the carboxylic group) forms two hydrogen bonds, the stronger intermolecular hydrogen bond between PA and SA weakens the intramolecular hydrogen bond. In contrast, the intramolecular hydrogen bond in PA-AM is stronger than that in PA. The adjacent O—H distance in PA-AM (0.992 Å) is longer than that in PA (0.986 Å), whereas the intramolecular hydrogen bond length in PA-AM (1.567 Å) is shorter than that in PA (1.598 Å). This is probably attributable to a weaker intermolecular hydrogen bond between PA and AM on the oxygen atom (O═C), leading to strengthening of the corresponding intramolecular hydrogen bond. The intramolecular hydrogen bond in PA-W is largely unaffected compared to that in PA, and the distances of the adjacent O—H and H···O intramolecular bonds are comparable between PA-W and PA. The geometrical features of the other heterodimer complexes of dicarboxylic acids with sulfuric acid/ammonia/water are similar and are comparable with those for monocarboxylic acids previously described by Zhao et al.[20]

In addition to the heterodimer molecular complexes, heterotrimer complexes of dicarboxylic acids with sulfuric acid/ammonia/water molecules are also investigated. Figure 4 depicts the optimized geometries of heterotrimer molecular

dx.doi.org/10.1021/jp301964u | J. Phys. Chem. A 2012, 116, 4539−4550

Table 1. Geometry Parameters and O—H Stretching Frequency for OA and MEA Calculated Using B3LYP/6-311++G(2d,2p)[a]

OA				MEA			
parameter	B3LYP/6-311++G(2d,2p)	PW91PW91/6-311++G(3df,3pd)[35]	exp[56]	parameter	B3LYP/6-311++G(2d,2p)	PW91PW91/6-311++G(3df,3pd)[35]	exp[55]
B_{C-C}	1.544	1.544	1.548	C1—O2	1.22	1.23	1.20
$B_{C=O}$	1.202	1.211	1.208	C1—O3	1.34	1.35	1.27
B_{C-O}	1.325	1.330	1.339	C1—C5	1.47	1.47	1.44
B_{O-H}	0.974	0.986	1.056	C5—C7	1.34	1.35	1.43
$A_{C-C=O}$	121.35	121.51	123.1	C7—C9	1.51	1.51	1.46
$A_{O=C-O}$	125.21	125.51	125.0	C9—C12	1.21	1.22	1.21
A_{C-O-H}	107.50	105.83	104.4	C9—C10	1.33	1.33	1.27
ν_{O-H}	3661	3487	3475	O2—O10	2.63	2.61	2.46
				O2—C1—O3	121.4	121.3	125.5
				O3—C1—C5	111.2	111.3	114.8
				O2—C2—O5	127.3	127.4	118.4
				C1—C5—C7	128.2	127.9	126.7
				C5—C7—C9	133.7	133.6	124.7
				C5—C7—C10	120.4	120.1	124.1
				O10—C9—O12	121.9	122.1	119.2
				C7—C9—O12	117.7	117.8	111.3

[a]Also included in the table for comparison are the experimental data[55] and results previously calculated using PW91PW91/6-311++G(3df,3pd).[34,35] The bond lengths, angles, and frequencies are given in angstroms, degrees, and cm^{-1}, respectively.

dx.doi.org/10.1021/jp301964u | J. Phys. Chem. A 2012, 116, 4539−4550

Table 2. Comparison of Vibrational Frequencies of MEA (cm^{-1}) among Calculated Using B3LYP/6-311++G(2d,2p), Previously Calculated Using PW91PW91/6-311++G(3df,3pd),[34,35] and the Experimental Values[57]

freq	B3LYP/6-311++G(2d,2p)	PW91PW91/6-311++G(3df,3pd)[34]	exp[57]
1	3756	3637	
2	3344	3132	
3	3199	3116	
4	3183	3091	
5	1785	1729	1705
6	1736	1678	1635
7	1676	1626	1587
8			1565
9	1461		1459
10	1449	1424	1432
11	1230	1297	1261
12	1178	1188	1218

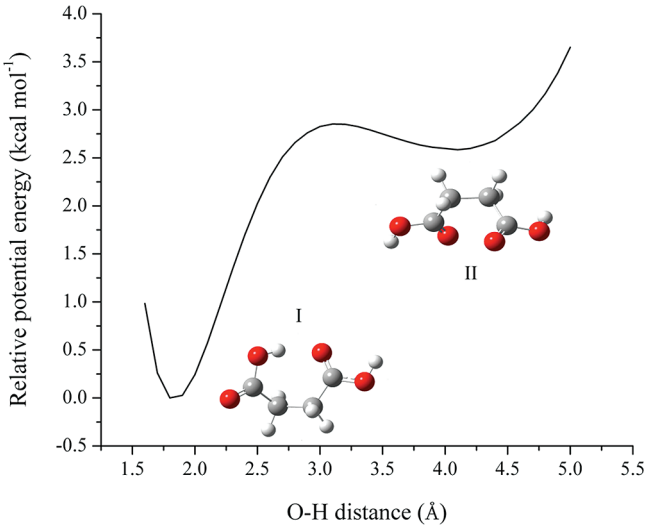

Figure 2. Potential energy surface along the intramolecular hydrogen bond obtained by the relaxed potential energy surface scan at B3LYP/6-311++G(2d,2p).

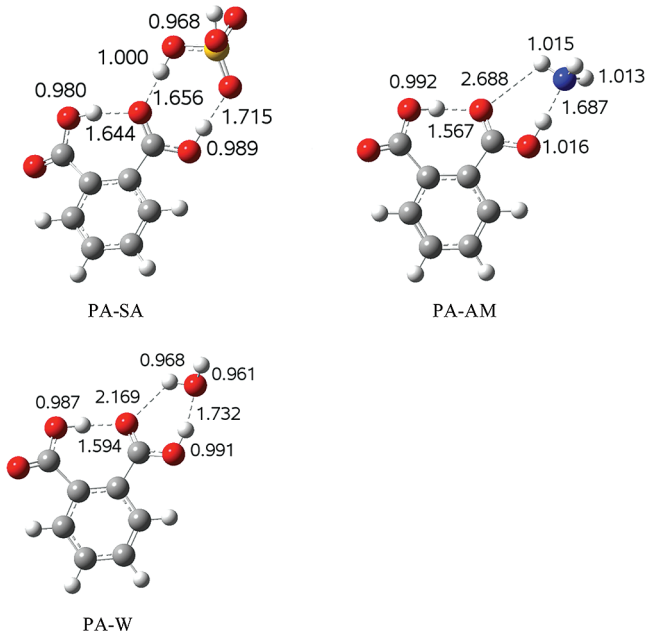

Figure 3. Optimized geometries of selected heterodimer complexes of phthalic acid with sulfuric acid, ammonia, and water at B3LYP/6-311++G(2d,2p).

complexes for selected dicarboxylic acids (SUA, OA, and PA). Those conformations are local minima on the multidimensional PES of the corresponding molecular clusters. More stable conformations may exist and be obtained by configurational sampling methods, which are out of the scope of this study. The heterotrimer complexes have two major configurations, one with dicarboxylic acids at the ends and another with dicarboxylic acids in the middle. For each configuration, the dicarboxylic acid has two major conformations. For example, in the SA-SUA-SA complex SUA has two conformations (I and II in Figure 4), with or without the intramolecular hydrogen bond. Both conformations I and II exhibit four hydrogen bonds. Conformation II is more stable than conformation I, because the weaker intramolecular hydrogen bond is replaced by a stronger SUA-SA intermolecular hydrogen bond. This finding is also corroborated by thermochemical analysis to be discussed in the next section.

The geometries of two heterotrimer complexes, SA-PA-SA and SA-PA-AM, can be compared with their corresponding heterodimer complexes. The four hydrogen bond lengths in SA-PA-SA complex are close to their counterparts in the SA-PA complex, except for the length of SO—H···O hydrogen bond. The lengths of two SO—H···O hydrogen bonds in SA-PA-SA are 1.574 and 1.588 Å, which are smaller than the length of the SO—H···O hydrogen bond (1.656 Å) in the SA-PA complex. Hence, the SO—H···O hydrogen bonds in SA-PA-SA are slightly stronger than the corresponding SO—H···O hydrogen bond in PA-SA. This is explainable because of weakening of the SO—H···O hydrogen bond by the adjacent intramolecular hydrogen bond in the PA-SA complex. The CO—H···O hydrogen bond lengths in SA-PA-SA are 1.735 and 1.725 Å, which are close to the length of CO—H···O hydrogen bond (1.715 Å) in PA-SA. This indicates the CO—H···O hydrogen bond strength is not affected by the intramolecular hydrogen bond in PA-SA. The strengths of the SO—H···O and CO—H···O hydrogen bonds on each side of SA-PA-SA are comparable, i.e., with the similar values of the hydrogen bond lengths on each side. For complex SA-PA-AM, the length of CO—H···N (1.717 Å) in SA-PA-AM is close to that of CO—H···N (1.687 Å) in PA-AM, whereas the length of NH···O (2.534 Å) in SA-PA-AM is smaller than that of NH···O (2.688 Å) in PA-AM. This suggests a small change of the NH···O hydrogen bond strength in PA-AM after addition of sulfuric acid on the other side, but the strength of CO—H···N

dx.doi.org/10.1021/jp301964u | J. Phys. Chem. A 2012, 116, 4539−4550

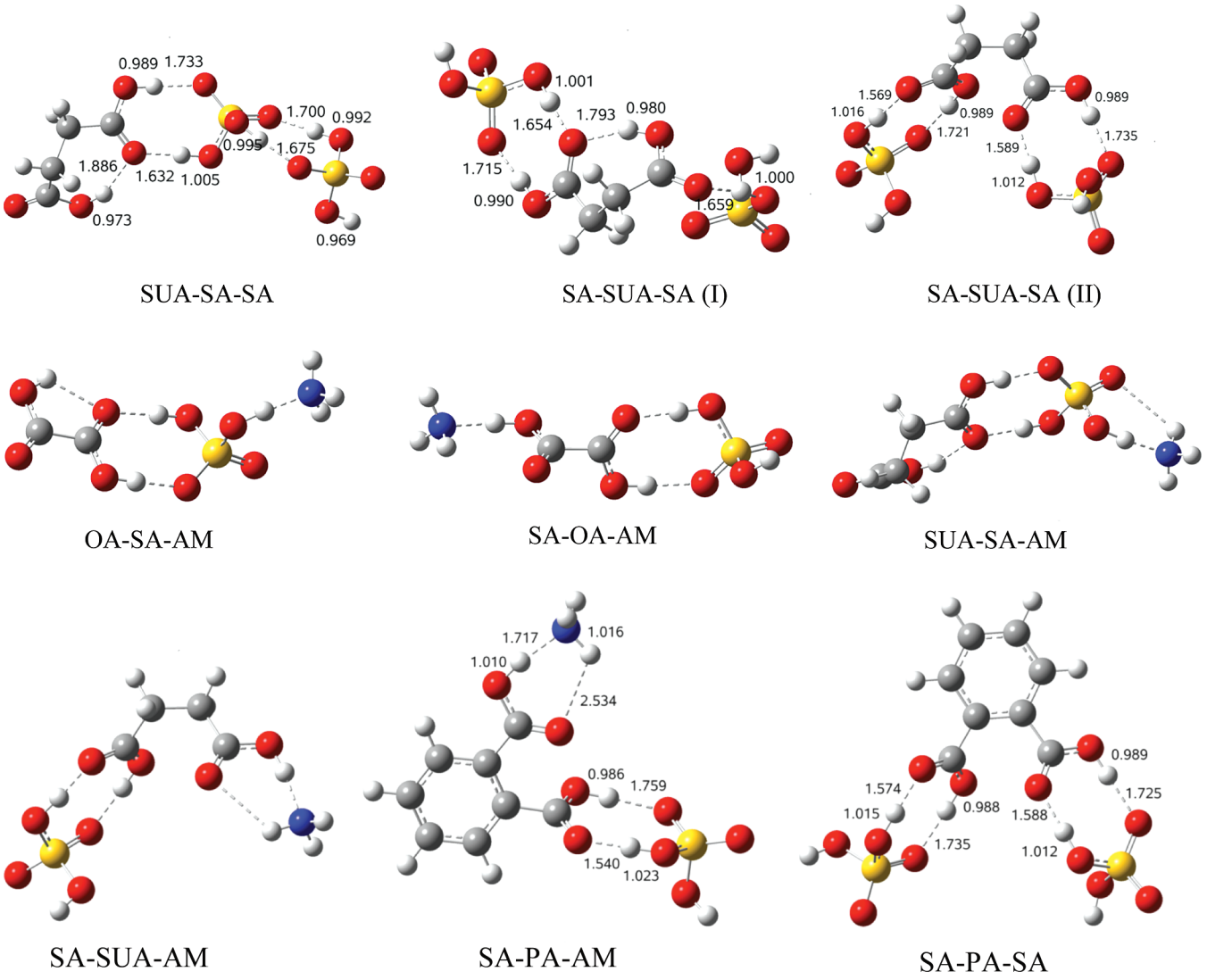

Figure 4. Optimized geometries of selected heterotrimer molecular complexes of dicarboxylic acids (i.e., phthalic, oxalic, and succinic acids) with sulfuric acid, ammonia, and water at B3LYP/6-311++G(2d,2p).

does not change noticeably after the sulfuric acid addition. The different characteristics in the CO—H···N and NH···O hydrogen bonds within the heterotrimer complex SA-PA-AM are attributable to the presence of the intramolecular hydrogen bond within the heterodimer complex PA-AM, similarly to those in the complex SA-PA-SA.

Formation of molecular complexes of dicarboxylic acids also results in changes of the vibrational frequencies of the functional groups. The values of the frequency shifts for the phthalic acid complexes are summarized in Table 3. Red shifts in stretching frequencies are evident for all the bonds that participate in the hydrogen bond formation. The amount of the red shift also reflects the strength of the hydrogen bonding. The SO—H···O═C (68.94 cm^{-1}) hydrogen bond is much stronger than the NH···O═C (29.78 cm^{-1}) and OH···O═C (26.38 cm^{-1}) hydrogen bonds, because the frequency shift of C═O stretching for the former hydrogen bond is much larger than that for the latter. Similarly, the COH···N (931.50 cm^{-1}) hydrogen bond is much stronger than the COH···O═S (414.18 cm^{-1}) and COH···O (451.89 cm^{-1}) hydrogen bonds. The interaction strength of phthalic acid with sulfuric acid/ammonia/water is determined by the combination of the two

Table 3. Frequency[a] (cm^{-1}) Shifts of the Functional Groups for Heterodimer and Heterotrimer Complexes of Phthalic Acid with Sulfuric Acid, Ammonia, and Water

complexes	S═O	SO—H	C═O	CO—H
PA-SA	−101.13	−651.15	−68.94	−414.18
PA-AM			−29.78	−931.50
PA-W			−26.38	−451.89
SA-PA-SA	−87.91	−847.39	−78.57	−386.24
	−92.19	−908.53	−84.46	−409.77
SA-PA-AM	−84.61	−1036.66	−83.05	−353.93
			−42.05	−819.32

[a]All frequencies are obtained from B3LYP/6-311++G(2d,2p) and are unscaled.

aforementioned hydrogen-bonding strengths. Red shifts in the stretching frequencies for O═C, O═S, CO—H, and SO—H functional groups also exist in the heterotrimer complexes. The values of the red shifts for the SA-PA-SA and SA-PA-AM heterotrimer complexes are also presented in Table 3. The frequency shifts of the two C═O functional groups in SA-PA-SA are 78.57 and 84.46 cm^{-1}, similar to the corresponding frequency

dx.doi.org/10.1021/jp301964u | J. Phys. Chem. A 2012, 116, 4539−4550

shift (68.94 cm^{-1}) in SA-PA. The frequency shifts of the two C═O functional groups in SA-PA-AM are 83.05 and 42.05 cm^{-1}, corresponding to those of 68.94 and 29.78 cm^{-1} in PA-SA and PA-AM, respectively. On the basis of the values of red shifts, it can be concluded that the interaction strength of dicarboxylic acids with sulfuric acid or ammonia in the heterotrimer complexes are comparable to that in the heterodimer complexes.

3.2. Topological and NBO Analysis. In addition to the geometrical analysis, topological analysis using QTAIM provides an alternative way to evaluate the hydrogen bond strength. According to Bader's theory, the nuclei are (3,−3) the critical points where the charge density is maximum in all directions. The bond critical points (BCP) (3,−1) correspond to the charge density Hessian matrix that has one positive and two negative eigenvalues. The bond critical points and the nuclei are connected by the maximum charge density paths. Two adjacent paths form a bond path by connecting the adjacent nuclei. The ring critical points (RCP) (3,+1) occur where the charge density Hessian has one negative and two positive eigenvalues. Nuclei, BCP, RCP, and bond paths constitute the molecular graphs, as presented in Figure 5. The ring structure of the inter- and intramolecular hydrogen bonds are similar to that described by Zhao et al.[20] The topological parameters, such as charge density (ρ) and its Laplacian ($\nabla^2\rho$), gradient kinetic energy density (G), potential energy density (V), and electronic energy density (K), are summarized in Table 4. The values of ρ, $\nabla^2\rho$, G, V, and K are comparable to those reported by Zhao et al.[20] A positive value of ρ indicates a closed-shell interaction between two hydrogen bonded atoms, according to Koch and Popelier.[46] The strength of the hydrogen bond is related to the magnitude of K at BCP of the corresponding hydrogen bond. The hydrogen bond strength increases with decreasing K. As a result, the intramolecular hydrogen bond strength increases from OA to SUA (−0.02 au) to MOA (−0.19 au) to MEA (−0.59 au) to PA (−0.88 au). Addition of sulfuric acid to PA (−0.57 au) decreases the intramolecular hydrogen bond strength, but addition of ammonia to PA (−1.17 au) increases the strength. However, addition of water to PA (−0.92 au) does not alter the strength appreciably. The strength of the stronger hydrogen bond in the complexes of PA with sulfuric acid, ammonia, and water decreases from PA-AM (−1.26 au) to PA-SA (−0.50 au) to PA-W (−0.28 au), whereas the strength of the weaker hydrogen bond in those clusters decreases from PA-SA (−0.21 au) to PA-W (0.17 au) to PA-AM. Those results are consistent with geometrical bond length analysis.

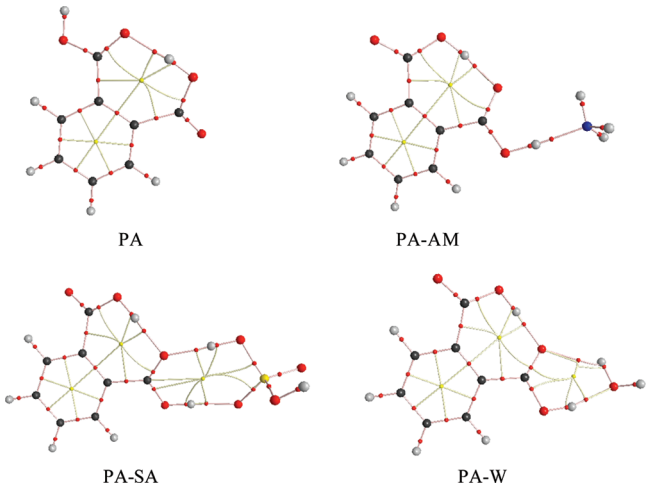

Figure 5. Molecular graphs of PA, PA-AM, PA-SA, and PA-W complexes showing the BCPs, ring critical points, bond path, and ring path.

In the NBO analysis, the hydrogen bond strength is related to the interaction energy between nonbonded natural orbital of the hydrogen acceptor and the unoccupied antibonding orbital of the hydrogen donor DH bond (σ^*_{DH}).[47] The interaction energies for those hydrogen bonds are summarized in Table 5. The intramolecular hydrogen bond strength increases in the order OA (2.42 kcal mol^{-1}), SUA (11.79 kcal mol^{-1}), MOA (16.05 kcal mol^{-1}), PA-SA (22.63 kcal mol^{-1}), MEA (27.03 kcal mol^{-1}), PA (31.31 kcal mol^{-1}), PA-W (31.43 kcal mol^{-1}), PA-AM (36.15 kcal mol^{-1}). On one hand, the strength of the stronger intermolecular hydrogen bond in the complexes of PA with sulfuric acid, ammonia, and water decreases from PA-AM (38.06 kcal mol^{-1}) to PA-SA (26.84 kcal mol^{-1}) to PA-W (21.18 kcal mol^{-1}). On the other hand, the strength of the weaker intermolecular hydrogen bond decreases from PA-SA (22.50 kcal mol^{-1}) to PA-W (2.05 kcal mol^{-1}) to PA-AM (0.10 kcal mol^{-1}). The combination of the two intermolecular hydrogen bonds strength shows that the interaction decreases

Table 4. Topological Parameters (Charge Densities, Laplacian, Gradient Kinetic Energy Densities, Potential Energy Densities, and Electronic Energy Densities) at BCPs of the Hydrogen Bonds of the Complexes (au)[a]

	$\rho(10^{-2})$	∇^2 (10^{-2})	$G(r)$ (10^{-2})	$V(r)$ (10^{-2})	$K(r)$ (10^{-2})	$\rho(10^{-2})$	∇^2 (10^{-2})	$G(r)$ (10^{-2})	$V(r)$ (10^{-2})	$K(r)$ (10^{-2})
			Inter HB							
MOA	3.99	12.20	3.24	−3.43	−0.19					
MEA	5.06	13.61	4.00	−4.59	−0.59					
PA	5.76	15.03	4.64	−5.53	−0.88					
SUA	3.26	10.27	2.59	−2.61	−0.02					
PA-SA	5.13	14.47	4.19	−4.77	−0.57					
PA-AM	6.28	15.27	4.98	−6.15	−1.17					
PA-W	5.84	15.06	4.69	−5.61	−0.92					
			Stronger HB					Weaker HB		
PA-SA	4.77	12.47	3.62	−4.12	−0.50	3.95	11.60	3.11	−3.33	−0.21
PA-AM	5.58	8.23	3.32	−4.58	−1.26					
PA-W	4.11	11.48	3.15	−3.44	−0.28	1.70	6.15	1.37	−1.20	0.17

[a]Geometries of all complexes are optimized at the B3LYP/6-311++G(2d,2p) level. The bond paths for the two intramolecular hydrogen bonds in OA and the weaker intermolecular hydrogen bond in PA-AM are not observed.

dx.doi.org/10.1021/jp301964u | J. Phys. Chem. A 2012, 116, 4539−4550

Table 5. NBO Interaction Energies[a] for the Hydrogen Bond of Different Complexes (kcal mol^{-1})

	inter HB	stronger HB	weaker HB
OA	2.42		
MOA	16.05		
MEA	27.03		
PA	31.31		
SUA	11.79		
PA-SA	22.63	26.84	22.25
PA-AM	36.15	38.06	0.10
PA-W	31.43	21.18	2.05

[a]All calculations are carried out at the B3LYP/6-311++G(2d,2p) level.

from PA-SA (49.34 kcal mol^{-1}) to PA-AM (38.16 kcal mol^{-1}) to PA-W (23.23 kcal mol^{-1}). This result further corroborates the findings in geometrical analysis and is consistent with the thermochemical analysis results, to be discussed in the next section.

3.3. Thermochemical Analysis. Table 6 summarizes the Gibbs free energy changes associated with hydration of sulfuric acid and oxalic acid and the complex formation involving sulfuric acid, ammonia, oxalic acid, and maleic acid. The B3LYP/6-311++G(2d,2p) results are also compared with those predicted by CCSD(T)/6-311++G(2d,2p) and previously reported using PW91PW91/6-311++G(3df,3pd).[34,35] The experimental value of the Gibbs free energy change of hydration of sulfuric acid is also included in Table 6 for comparison. For hydration of sulfuric acid, the B3LYP value (−1.00 kcal mol^{-1}) is about 1 kcal mol^{-1} higher than those of PW91PW91 (−2.28 kcal mol^{-1}) and CCSD(T) (−2.23 kcal mol^{-1}). After the BSSE correction, the B3LYP and CCSD(T) values are similar, but smaller than that of PW91PW91. Note for sulfuric acid hydration, the BSSE method yields a more positive value, which differs further from the experimental value (−3.60 kcal mol^{-1}).[48] It has been previously suggested that the BSSE correction may not necessarily improve the accuracy in energetic predictions for molecular complexes, as previously explained by Kurtén et al.[32] For hydration of oxalic acid, the B3LYP value (0.77 kcal mol^{-1}) is higher than those predicted by CCSD(T) (0.23 kcal mol^{-1}) and PW91PW91 (−1.17 kcal mol^{-1}). After the BSSE correction, the B3LYP (1.42 kcal mol^{-1}) and CCSD(T) (2.42 kcal mol^{-1}) values are higher than that of PW91PW91. Currently, there exists no experimental value of Gibbs free energy changes associated with hydration for dicarboxylic acids in the literature. Herb et al.[49] indicated that a comparison of the DFT methods against a high level of ab initio method may not be useful, because few ab inito predictions of stepwise Gibbs free energy changes have been studied systematically and validated against experimental values. Also, the determination of experimental enthalpies typically employes the linearized van't Hoff equation, which may introduce additional error.[49]

All thermal properties are calculated at the B3LYP level with a 6-311++G(2d,2p) basis set at 1 atm and 298.15 K. The changes in the electronic energy (with the zero point energy, ZPE, correction), enthalpy, free energy, BSSE, and PW91PW91 corrected free energy of the reaction for the heterodimer complexes are summarized in Table 7. The PW91PW91 method consistently predict the energy of about 2.00 kcal mol^{-1} lower than that by B3LYP without BSSE correction. From the electronic energy (with ZPE) changes, the interaction strength of the dicarboxylic acid with sulfuric acid/ammonia/water at 0 K is determined. For the phthalic acid complexes, the interaction of PA with sulfuric acid (−12.69 kcal mol^{-1}) is much stronger than those with ammonia (−10.87 kcal mol^{-1}) and water (−7.91 kcal mol^{-1}), consistent with the previous results of Zhao et al.[20] The geometrical, topological, and NBO analysis shows that PA-SA has one strong hydrogen bond and one medium strength hydrogen bond. In contrast, PA-AM and PA-W have one strong hydrogen bond and one weak hydrogen bond, and the strong hydrogen bond in PA-AM is stronger than that in PA-W.

To obtain the thermochemical properties of the molecular complexes under atmospheric conditions, the temperature effect needs to be taken into account. At 298.15 K, the interaction of dicarboxylic acids with sulfuric acid/ammonia/water includes the contributions from the translational, rotational and vibrational energies, and the thermochemical properties of the molecular complexes are related to enthalpy and entropy. If only enthalpy is considered, the interaction of PA with sulfuric acid is the strongest, followed by those with ammonia and water, because the enthalpy changes of reaction are −12.51, −11.13, and −8.40 kcal mol^{-1} for PA-SA, PA-AM, and PA-W, respectively. However, when incorporating the

Table 6. Changes of Gibbs Free Energy (kcal mol^{-1}) for Complex Formation by Sulfuric Acid, Organic Acids, Ammonia, and Water with and without (in Parentheses) BSSE Calculated Using B3LYP, PW91PW91, and CCSD(T) with Two Basis Sets, i.e., 6-311++G(2d,2p) and 6-311++G(3df,3pd)[a]

	B3LYP/ 6-311++G(2d,2p)	PW91PW91/6-311++G(3df,3pd)// B3LYP/6-311++G(2d,2p)	CCSD(T)/6-311++G(3df,3pd)// B3LYP/6-311++G(2d,2p)	PW91PW91/ 6-311++(3df,3pd)[34,35]	exp
SA + W ⇔ SA-W	−1.00 (−0.300)	−2.72 (−1.97)	−2.23 (−0.13)	−2.28	−3.6 ± 1.0
SA + AM ⇔ SA-AM	−5.56 (−4.99)	−7.90		−7.77	
SA + SA ⇔ SA-SA	−3.35 (−2.23)	−5.65		−5.59	
OA + W ⇔ OA-W	0.77 (1.42)	−1.17 (−0.47)	0.23 (2.42)	−0.96	
OA + AM ⇔ OA-AM	−2.23 (−1.74)	−4.55		−4.42	
OA + SA ⇔ OA-SA	−0.71 (0.19)	−2.74		−3.24	
MEA + AM ⇔ MEA-AM	−3.14 (−3.04)	−5.01		−5.34	
MEA + SA ⇔ MEA-SA	−2.12 (−1.45)	−4.58		−4.89	

[a]Also included in the table for comparison are the experimental data[48] of hydration of sulfuric acid and results previously calculated using PW91PW91/6-311++G(3df,3pd).[34,35]

dx.doi.org/10.1021/jp301964u | J. Phys. Chem. A 2012, 116, 4539−4550

Table 7. Electronic Energy of Reaction (ΔE) (with ZPE), Enthalpy of Reaction (ΔH), Free Energy of Reaction (ΔG) for Heterodimer Complexes, and BSSE Corrected Free Energy of Reactions[a]

reaction/energy	ΔE(ZPE)	ΔH	ΔG	ΔS^b	ΔG(BSSE)	ΔG(PW91PW91/6-311++G(3df,3pd)//B3LYP/6-311++G(2d,2p))
SA + AM ⇔ SA-AM	−13.27	−13.74	−5.56	−27.43	−4.99	−7.90
OA + AM ⇔ OA-AM	−9.01	−9.23	−2.23	−25.71	−1.14	−4.55
MOA + AM ⇔ MOA-AM	−10.98	−11.29	−2.86	−28.28	−2.43	−4.93
MEA + AM ⇔ MEA-AM	−11.24	−11.54	−3.14	−28.19	−3.04	−5.01
PA + AM ⇔ PA-AM	−10.87	−11.13	−2.65	−28.44	−2.25	−4.78
SUA + AM ⇔ SUA-AM	−10.52	−10.83	−2.33	−28.51	−1.93	−4.51
SA + SA ⇔ SA-SA	−13.14	−13.14	−3.35	−32.84	−2.23	−5.65
OA + SA ⇔ OA-SA	−10.29	−10.14	−0.71	−32.90	0.59	−2.74
MOA + SA ⇔ MOA-SA	−12.73	−12.67	−1.86	−36.23	−0.93	−4.23
MEA + SA ⇔ MEA-SA	−12.58	−12.45	−2.12	−34.63	−1.45	−4.58
PA + SA ⇔ PA-SA	−12.69	−12.51	−2.11	−34.87	−1.02	−4.37
SUA + SA ⇔ SUA-SA	−12.82	−12.68	−2.43	−34.39	−1.47	−4.93
SA + W ⇔ SA-W	−9.06	−9.71	−1.00	−29.19	−0.30	−2.72
OA + W ⇔ OA-W	−5.51	−5.95	0.77	−27.94	2.95	−1.17
MOA + W ⇔ MOA-W	−7.81	−8.36	1.00	−31.40	1.56	−0.58
MEA + W ⇔ MEA-W	−7.98	−8.48	0.53	−30.24	0.81	−1.07
PA + W ⇔ PA-W	−7.91	−8.40	0.74	−30.63	1.31	−1.06
SUA + W ⇔ SUA-W	−7.60	−8.12	0.92	−30.31	1.48	−0.70

[a]Energy in kcal mol^{-1} at the B3LYP/6-311++G(2d,2p) level. [b]Entropy in cal mol^{-1} K^{-1} at the B3LYP/6-311++G(2d,2p) level.

entropy changes, the interaction of PA with ammonia (−2.25 kcal mol^{-1}) becomes the strongest, followed by those with sulfuric acid (−1.02 kcal mol^{-1}) and water (1.31 kcal mol^{-1}). The entropy changes also consist of the translational, rotational, and vibrational entropy components, and the values of the translational, rotational, and vibrational entropies for the complexes between PA with sulfuric acid, ammonia, and water are listed in Table 8. The translational entropy changes

Table 8. Translational (ΔS_{tr}), Rotational (ΔS_{rot}), Vibrational (ΔS_{vib}), and Total (ΔS_{total}) Entropy Changes of Reaction (cal mol^{-1} K^{-1}) for Heterodimer and Heterotrimer Complexes of Phthalic Acid with Sulfuric Acid, Ammonia, and Water at the B3LYP/6-311++G(2d,2p) Level

complex	ΔS_{tr}	ΔS_{rot}	ΔS_{vib}	ΔS_{total}
PA-AM	−34.15	−10.42	16.12	−28.45
PA-SA	−38.27	−20.92	24.32	−34.87
PA-W	−34.30	−9.48	13.15	−30.63
SA-PA-SA[a]	−38.72	−21.86	26.68	−33.90
SA-PA-AM[b]	−34.26	−10.81	18.35	−26.71

[a]SA-PA-SA is formed through the association reaction of SA-PA with SA. [b]SA-PA-AM is formed through the association reaction of SA-PA with AM.

represent the most important term in the total entropy changes; this arises because the number of molecules decreases from two for the heterodimer complex to one for the PA monomer in the association reaction. The changes in the rotational and vibrational entropy nearly cancel out each other. Because the translational entropy depends not only on the temperature but also on the number concentration of the molecules, the relative stability of the PA-SA, PA-AM, and PA-W complexes varies with the concentrations of those species in the atmosphere. At the concentrations corresponding to 1 atm and 298.15 K, the total entropy changes are practically independent of the structures of the molecules and only vary with the type of interaction, i.e., about −34 cal mol^{-1} K^{-1} for SA with dicarboxylic acids, about −28 cal mol^{-1} K^{-1} for ammonia with dicarboxylic acids, and −30 cal mol^{-1} K^{-1} for water with dicarboxylic acids. The entropy changes for the heterotrimer complexes, SA-PA-SA and SA-PA-AM, are also presented in Table 9. The total entropy changes of reaction for the SA-PA-SA (−33.90 cal mol^{-1} K^{-1}) and SA-PA-AM (−26.71 cal mol^{-1} K^{-1}) complexes are close to those for PA-SA (−34.87 cal mol^{-1} K^{-1}) and PA-AM (−28.45 cal mol^{-1} K^{-1}), indicating that the interaction of PA with SA and AM in heterotrimer complexes is similar to that in the corresponding heterodimer complexes.

The thermochemical properties of the heterotrimer complexes are presented in Table 9. The complexes of SUA with two sulfuric acid molecules are discussed to illustrate the heterotrimer interaction. There are two possible interactions in the heterotrimer complexes, i.e., SA-SUA-SA and SUA-SA-SA. For SA-SUA-SA, two conformations are obtained from the geometry optimization. The free energy for conformation II is lower than that for conformation I. There exists no intramolecular hydrogen bond within the succinic acid molecule for conformation II, but in conformation I succinic acid retains its intramolecular hydrogen bond, consistent with discussion in the Geometrical Analysis section. The enthalpies of reaction for heterotrimer complexes are similar to those for heterodimer complexes. For example, the enthalpy of reaction for PA-AM (−11.13 kcal mol^{-1}) is close to that for SA-PA-AM (−12.56 kcal mol^{-1}) from the association reaction of SA-PA and AM. This implies that the formation of heterotrimer complexes from heterodimer complexes is as favorable as that of heterodimer complexes.

The thermochemical analysis may be subject to a possible error caused by the approximation of the internal rotor using harmonic oscillator. To quantify this effect, hindered internal

dx.doi.org/10.1021/jp301964u | J. Phys. Chem. A 2012, 116, 4539−4550

Table 9. Electronic Energy (ΔE), Enthalpy (ΔH), Free Energy (ΔG), and Entropy Changes of Reaction (ΔS) for Heterotrimer Molecular Complexes[a]

reaction	ΔE(ZPE)	ΔH	ΔG(B3LYP)	ΔS	ΔG(PW91PW91/6-311++G(3df,3pd)//B3LYP/6-311++G(2d,2p))
SA + OA-SA ⇔ SA-OA-SA	−10.40	−9.94	−0.11	−31.72	−1.85
SA + OA-SA ⇔ OA-SA-SA	−13.27	−13.12	−3.14	−32.23	−5.68
SA + SUA-SA ⇔ SA-SUA-SA(I)	−11.73	−11.43	−1.72	−32.57	−2.94
SA + SUA-SA ⇔ SA-SUA-SA(II)	−18.64	−18.49	−8.44	−33.69	−9.71
SA + SUA-SA ⇔ SUA-SA-SA	−13.26	−13.24	−2.93	−34.55	−5.27
W + OA-SA ⇔ OA-SA-W	−9.32	−9.84	−0.90	−28.69	−2.64
W + OA-SA ⇔ W-OA-SA	−7.50	−7.87	1.01	−28.53	−0.42
W + SUA-SA ⇔ W-SUA-SA(I)	−3.40	−3.39	3.04	−21.56	2.18
W + SUA-SA ⇔ W-SUA-SA(II)	−11.19	−11.71	−3.06	−29.00	−4.31
W + SUA-SA ⇔ SUA-SA-W	−9.35	−9.97	−0.97	−30.22	−2.79
OA-SA + AM ⇔ OA-SA-AM	−14.49	−15.00	−6.05	−28.76	−8.81
OA-SA + AM ⇔ SA-OA-AM	−11.08	−11.16	−3.83	−23.34	−5.83
SUA-SA + AM ⇔ SUA-SA-AM	−14.16	−14.70	−5.90	−29.50	−8.58
SUA-SA + AM ⇔ SA-SUA-AM	−13.43	−13.62	−5.62	−26.86	−7.22
PA-SA + AM ⇔ SA-PA-AM	−12.47	−12.56	−4.59	−26.71	−6.01
PA-SA + SA ⇔ SA-PA-SA	−17.70	−17.41	−7.31	−33.90	−9.33
PA-AM + SA ⇔ SA-PA-AM	−14.30	−13.93	−4.05	−33.14	−5.61

[a]The thermal data are from B3LYP/6-311++G(2d,2p) calculation. Energy is in kcal mol^{-1}. Entropy is in cal mol^{-1} K^{-1}.

rotor analysis is carried out for PA using Gaussian 03 package.[39] McClurg's[50,51] free energy correction of 0.02 kcal mol^{-1} is 1 order of magnitude smaller than that reported by Ehn et al. (0.5 kcal mol^{-1}).[36] Hence, the harmonic approximation of internal rotor does not introduce a significant error in our study. Another possible source of errors includes neglecting the gas-phase hydration effect,[52] which may be important for complex formation in the atmosphere and will be assessed in future studies. It should also be pointed out that the concentrations of the aerosol precursors (excluding water vapor) in the atmosphere are relatively small and the equilibrium for the formation of the prenucleation molecular complexes is rarely established. Hence, cautions need to be exercised to predict the equilibrium distributions of those prenucleation molecular complexes using the theoretically predicted free energies and the gaseous concentrations of sulfuric acid, ammonia, and organic acids. Furthermore, the free energies predicted in Tables 7 and 9 do not account for the liquid-like properties for the pre-nucleation molecular complexes, in particular, when the size of the complexes is large. For example, there typically exists a nucleation barrier, as demonstrated in supersaturation phenomenon, to over-come the entropy restriction during the initial stage of a phase transformation (i.e., vapor to liquid, vapor to solid, or liquid to solid).[9] The quantum chemical calculations likely overestimate the translational entropy by treating the prenucleation molecular clus-ters as ideal gases. Indeed, the free energies predicted by quantum chemical calculations fail to exhibit an activation barrier, in contrast to that predicted by the classical nucleation theory, as discussed analogously by Reiss et al. on the translational-rotational paradox.[53]

4. CONCLUSIONS

DFT, QTAIM, and NBO methods have been applied to investigate the interaction of selected dicarboxylic acids (i.e., oxalic acid, malonic acid, maleic acid, phthalic acid, and succinic acid) with common atmospheric aerosol nucleation precursors (i.e., sulfuric acid, ammonia, and water). The B3LYP density functional with 6-311++G(2d,2p) basis set is applied to obtain the energetics of the molecular cluster formation. Comparisons are made between the predictions using several different theoretical methods and with the experimental results. The geometrical, topological, and NBO analysis shows that the dicarboxylic−sulfuric acid complex has one strong hydrogen bond and one medium strength hydrogen bond, similar to those monocarboxylic acids previously reported.[20] The heterodimer interaction shows that at 0 K dicarboxylic acids have the strongest interactions with sulfuric acid, followed by those with ammonia and water. At room temperature, due to the contribution from entropy changes of reaction, dicarboxylic acids have the strongest interaction with ammonia, followed by those with sulfuric acid and water. The heterotrimer interaction shows that dicarboxylic acids bind with two sulfuric acid molecules, and the resulting complex is hydrophilic in both ends. The geometrical analysis of the heterotrimer dicarboxylic acid−sulfuric acid complexes exhibit characteristics similar to those of the heterodimer dicarboxylic acid complexes, i.e., with one strong hydrogen bond and one medium strength hydrogen bond on each side of the carboxylic functional group. The enthalpies of reaction for heterotrimer complexes are similar to those for heterodimer complexes, indicating that the formation of heterotrimer complexes from heterodimer complexes is as favorable as that of heterodimer complexes.

Sulfuric acid has been commonly considered as a key species in atmospheric new particle formation.[7] However, it well recognized that the atmospheric concentration of gas-phase sulfuric acid is typically too low to explain nucleation and growth of atmospheric nanoparticles.[7,54] Binary nucleation of the sulfuric acid/water system alone is insufficient to explain nucleation rates observed in field measurements of diverse environmental conditions, i.e., urban, rural, remote continental, free troposphere, and coastal areas. Monocarboxylic acids, formed from photochemical oxidation of anthropogenic and biogenic hydrocarbons have been identified as an important

element in the aerosol nucleation process.[15,17] Oxalic acid, malonic acid, maleic acid, phthalic acid, and succinic acid investigated in this study are the most abundant forms of dicarboxylic acids in the atmosphere. The free energies of formation of the heterodimer and heterotrimer clusters suggest that dicarboxylic acids can contribute to the aerosol nucleation process by binding to sulfuric acid and ammonia. In particular, the formation energies and structures of the heterotrimer clusters show that dicarboxylic acids enhance nucleation in two directions, in contrast to monocarboxylic acids. As a result, the heterodimer and heterotrimer complexes of dicarboxylic acids likely act as the linking elements in sulfuric acid/ammonia/water nucleation. Future experimental studies are required to investigate the contribution of dicarboxylic acids to aerosol nucleation under atmospheric conditions.

■ ASSOCIATED CONTENT

Supporting Information

Includes the tables for electronic energy, enthalpy, free energy of different species and a comparison of the calculated sulfuric acid, ammonia, and water geometries with the experimental geometries. This material is available free of charge via the Internet at http://pubs.acs.org.

■ AUTHOR INFORMATION

Corresponding Author

*E-mail: Renyi-zhang@tamu.edu. Fax: +979-862-4466.

Notes

The authors declare no competing financial interest.

■ ACKNOWLEDGMENTS

This work was supported the Robert A. Welch Foundation (Grant A-1417) and the US National Science Foundation (AGS-0938352). Additional support was provided by the Texas A&M University Supercomputing Facilities. We thank the Laboratory for Molecular Simulations at Texas A&M University and Dr. Lisa M. Pérez for assistance.

■ REFERENCES

(1) Solomon, S.; Qin, D.; Manning, M.; Chen, Z.; Marquis, M.; Averyt, K. B.; Tignor, M.; Miller, H. L. In *Climate Change 2007: The Physical Science Basis. Contribution of Working Group I to the Fourth Assessment Report of the Intergovernmental Panel on Climate Change*; Cambridge University Press: Cambridge, United Kingdom, and New York, NY, USA, 2007.

(2) *EPA Air quality criteria for particulate matter*; U.S. Environmental Protection Agency: Washington, DC, 2004.

(3) Zhang, R. Y.; Li, G. H.; Fan, J. W.; Wu, D. L.; Molina, M. J. *Proc. Natl. Acad. Sci. U. S. A.* **2007**, *104*, 5295−5299.

(4) Molina, M. J.; Molina, L. T.; Zhang, R. Y.; Meads, R. F.; Spencer, D. D. *Geophys. Res. Lett.* **1997**, *24*, 1619−1622.

(5) Zhang, R. Y.; Leu, M. T.; Molina, M. J. *Geophys. Res. Lett.* **1996**, *23*, 1669−1672.

(6) Li, G. H.; Zhang, R. Y.; Fan, J. W.; Tie, X. X. *J. Geophys. Res.* **2005**, *110*, D23206; DOI: 10.1029/2005JD005898.

(7) Zhang, R. Y. *Science* **2010**, *328*, 1366−1367.

(8) Wang, L.; Khalizov, A. F.; Zheng, J.; Xu, W.; Ma, Y.; Lal, V.; Zhang, R. Y. *Nat. Geosci.* **2010**, *3*, 238−242.

(9) Zhang, R.; Khalizov, A.; Wang, L.; Hu, M.; Xu, W. *Chem. Rev.* **2012**, *112*, 1957−2011.

(10) Yue, D. L.; Hu, M.; Zhang, R. Y.; Wang, Z. B.; Zheng, J.; Wu, Z. J.; Wiedensohler, A.; He, L. Y.; Huang, X. F.; Zhu, T. *Atmos. Chem. Phys.* **2010**, *10*, 4953−4960.

(11) Ball, S. M.; Hanson, D. R.; Eisele, F. L.; McMurry, P. H. *J. Geophys. Res.* **1999**, *104*, 23709−23718.

(12) Young, L. H.; Benson, D. R.; Kameel, F. R.; Pierce, J. R.; Junninen, H.; Kulmala, M.; Lee, S. H. *Atmos. Chem. Phys.* **2008**, *8*, 4997−5016.

(13) Yu, F.; Turco, R. P. *J. Geophys. Res.* **2001**, *106*, 4797−4814.

(14) Lee, S.-H.; Reeves, J. M.; Wilson, J. C.; Hunton, D. E.; Viggiano, A. A.; Miller, T. M.; Ballenthin, J. O.; Lait, L. R. *Science* **2003**, *301*, 1886−1889.

(15) Zhang, R.; Suh, I.; Zhao, J.; Zhang, D.; Fortner, E. C.; Tie, X.; Molina, L. T.; Molina, M. J. *Science* **2004**, *304*, 1487−1490.

(16) Fan, J.; Zhang, R.; Collins, D.; Li, G. *Geophys. Res. Lett.* **2006**, *33*, L15802 DOI: 10.1029/2006GL026295.

(17) Zhang, R. Y.; Wang, L.; Khalizov, A. F.; Zhao, J.; Zheng, J.; McGraw, R. L.; Molina, L. T. *Proc. Natl. Acad. Sci. U. S. A.* **2009**, *106*, 17650−17654.

(18) Zheng, J.; Khalizov, A. F.; Wang, L.; Zhang, R. *Anal. Chem.* **2010**, *82*, 7302−7308.

(19) Nadykto, A. B.; Yu, F. Q. *Chem. Phys. Lett.* **2007**, *435*, 14−18.

(20) Zhao, J.; Khalizov, A.; Zhang, R. Y.; McGraw, R. *J. Phys. Chem. A* **2009**, *113*, 680−689.

(21) Zhao, J.; Zhang, R.; Misawa, K.; Shibuya, K. *J. Photochem. Photobiol. A* **2005**, *176*, 199−207.

(22) Zhang, D.; Lei, W. F.; Zhang, R. Y. *Chem. Phys. Lett.* **2002**, *358*, 171−179.

(23) Lei, W. F.; Zhang, R. Y. *J. Phys. Chem. A* **2001**, *105*, 3808−3815.

(24) Zhao, J.; Levitt, N. P.; Zhang, R. Y.; Chen, J. M. *Environ. Sci. Technol.* **2006**, *40*, 7682−7687.

(25) Zhao, J.; Levitt, N. P.; Zhang, R. Y. *Geophys. Res. Lett.* **2005**, *32*, L09802 DOI: 10.1029/2004GL022200.

(26) Hoffmann, T.; Bandur, R.; Marggraf, U.; Linscheid, M. *J. Geophys. Res.* **1998**, *103*, 25569−25578.

(27) McGraw, R.; Zhang, R. Y. J. *Chem. Phys.* **2008**, *128*, 064508 DOI: 10.1063/1.2830030.

(28) Kurten, T.; Torpo, L.; Ding, C. G.; Vehkamaki, H.; Sundberg, M. R.; Laasonen, K.; Kulmala, M. *J. Geophys. Res.-Atmos.* **2007**, *112*, D04210.

(29) Kurtén, T.; Torpo, L.; Sundberg, M. R.; Kerminen, V. M.; Vehkamäki, H.; Kulmala, M. *Atmos. Chem. Phys.* **2007**, *7*, 2765−2773.

(30) Loukonen, V.; Kurten, T.; Ortega, I. K.; Vehkamaki, H.; Padua, A. A. H.; Sellegri, K.; Kulmala, M. *Atmos. Chem. Phys.* **2010**, *10*, 4961−4974.

(31) Nadykto, A.; Yu, F.; Jakovleva, M.; Herb, J.; Xu, Y. *Entropy* **2011**, *13*, 554−569.

(32) Kurtén, T. *Entropy* **2011**, *13*, 915−923.

(33) Sloth, M.; Bilde, M.; Mikkelsen, K. V. *Mol. Phys.* **2004**, *102*, 2361−2368.

(34) Xu, Y.; Nadykto, A. B.; Yu, F.; Herb, J.; Wang, W. *J. Phys. Chem. A* **2009**, *114*, 387−396.

(35) Xu, Y.; Nadykto, A. B.; Yu, F.; Jiang, L.; Wang, W. *J. Mol. Struct.: THEOCHEM* **2010**, *951*, 28−33.

(36) Ehn, M.; Junninen, H.; Petäjä, T.; Kurtén, T.; Kerminen, V. M.; Schobesberger, S.; Manninen, H. E.; Ortega, I. K.; Vehkamäki, H.; Kulmala, M.; et al. *Atmos. Chem. Phys.* **2010**, *10*, 8513−8530.

(37) Paul A, M. *Atmos. Environ.* **2001**, *35*, 961−974.

(38) Chebbi, A.; Carlier, P. *Atmos. Environ.* **1996**, *30*, 4233−4249.

(39) Frisch, M. J.; Trucks, G. W.; Schlegel, H. B.; Scuseria, G. E.; Robb, M. A.; Cheeseman, J. R.; Montgomery, J. A.; Vreven, T.; Kudin, K. N.; Burant, J. C.; et al. *Gaussian 03*, Revision C.02; Gaussian Inc.: Wallingford, CT, 2003.

(40) Bader, R. F. W. *Atoms in Molecules: a quantum theory*; Clarendon Press: Oxford, U.K., 1990.

(41) Biegler-König, F. *J. Comput. Chem.* **2000**, *21*, 1040−1048.

(42) Biegler-König, F.; Schönbohm, J.; Bayles, D. *J. Comput. Chem.* **2001**, *22*, 545−559.

(43) Biegler-König, F.; Schönbohm, J. *J. Comput. Chem.* **2002**, *23*, 1489−1494.

(44) Reed, A. E.; Curtiss, L. A.; Weinhold, F. *Chem. Rev.* **1988**, *88*, 899−926.

(45) Price, D. J.; Roberts, J. D.; Jorgensen, W. L. *J. Am. Chem. Soc.* **1998**, *120*, 9672−9679.
(46) Koch, U.; Popelier, P. L. A. *J. Phys. Chem.* **1995**, *99*, 9747−9754.
(47) Wendler, K.; Thar, J.; Zahn, S.; Kirchner, B. *J. Phys. Chem. A* **2010**, *114*, 9529−9536.
(48) Hanson, D. R.; Lovejoy, E. R. *J. Phys. Chem. A* **2006**, *110*, 9525−9528.
(49) Herb, J.; Nadykto, A. B.; Yu, F. *Chem. Phys. Lett.* **2011**, *518*, 7−14.
(50) McClurg, R. B.; Flagan, R. C.; W., A. G., III. *J. Chem. Phys.* **1997**, *106*, 6675−6680.
(51) McClurg, R. B. *J. Chem. Phys.* **1998**, *108*, 1748−1749.
(52) Nadykto, A. B.; Yu, F.; Herb, J. *Chem. Phys.* **2009**, *360*, 67−73.
(53) Reiss, H.; Katz, J. L.; Cohen, E. R. *J. Chem. Phys.* **1968**, *48*, 5553−5560.
(54) Zheng, J.; Hu, M.; Zhang, R.; Yue, D.; Wang, Z.; Guo, S.; Li, X.; Bohn, B.; Shao, M.; He, L.; et al. *Atmos. Chem. Phys.* **2011**, *11*, 7755−7765.
(55) Shahat, M. *Acta Crystallogr.* **1952**, *1952*, 763−768.
(56) Derissen, J. L.; Smith, P. H. *Acta Crystallogr., Sect. B* **1974**, *30*, 2240−2242.
(57) Beyer, K. D.; Friesen, K.; Bothe, J. R.; Palet, B. *J. Phys. Chem. A* **2008**, *112*, 11704−11713.